6. The proton NMR data (Bruker AC-100, $CDCl_3$, δ) of the key intermediary products are as follows; for **1**, 1.3 (3H, s), 1.6 (3H, m), 2.3 (5H, m), 5.5 (1H, br.s), 6.8 (2H, m), 7.3 (1H, m), 8.1 (1H, dd), 12.6 (1H, s); **2** 1.3 (3H, s), 1.6 (3H, m), 2.4 (4H, m), 3.8 (3H, s), 5.5 (1H, br.s), 6.9 (3H, m), 7.3 (1H, m); **6**, 1.2 (3H, t), 1.3 (3H, s), 1.5 (3H, m), 2.3 (4H, m), 4.1 (2H, q), 5,4 (1H, br.s); and **8**, 1.2 (3H, s), 1.6 (3H, m), 2.3 (4H, m), 5.6 (1H, br.s), 9.4 (1H, s).
7. Murov, S. L. *Handbook of Photochemistry*; Marcel Dekker: New York, 1973; p 125.

Asymmetric Metal-Insulator Transitions and Low Magnetic Field Giant Magnetoresistance of $Sm_{1-x}Sr_xMnO_3$ ($0.35 \leq x \leq 0.5$)

Eun Ok Chi, Jae-Kyoung Kang, Young-Uk Kwon, and Nam Hwi Hur†

Department of Chemistry, Sung Kyun Kwan University, Suwon 440-746, Korea
†Korea Research Institute of Science and Standards, Taejon 305-600, Korea
Received August 27, 1997

The giant magnetoresistance (GMR) properties of mixed valent perovskite-type manganese oxides are attracting wide attention partly due to the hope of developing better MR materials.[1-4] However, despite the impressively large MR values, most of known compounds of this class has significant demerits for such applications. They generally require very strong magnetic fields to exhibit significant MR effects and the temperatures for the maximum MR are usually far below room temperature. The first problem is considered to be more serious for realization of manganese oxide based MR devices.[1-3,5-7]

Previously, we have studied many perovskite type manganese oxides for their electrical properties and have related their metal-insulator (MI) transitions to the lattice distortions created by the A-site cation sizes of the general formula ABO_3.[8] During this work, we found that compounds in the $Sm_{1-x}Sr_xMnO_3$ system had asymmetric peaks in the resistivity *vs.* temperature plots with sharp changes of resistivity with temperature below T_{MI}'s. Since application of magnetic field raises T_{MI} and thereby lowers the resistivity particularly at around T_{MI}, we thought that such sharp transitions would result in large MR ratios.

Recently, Tokura *at al.* reported a lattice striction coupled MR in a perovskite type $(Nd_{1-y}Sm_y)_{1/2}Sr_{1/2}MnO_3$ (y=0.938) single crystal.[9] This compound exhibits simultaneous ferromagnetic ordering, MI transition and lattice shrinkage at T_{MI}. The resistance rises almost vertically with temperature by an order of 10^3 ohm·cm just below T_{MI}, and consequently, this compound shows a large MR effect of almost 100% under as low applied field as 0.25 T. Similar MI transitions are observed in the other members of the solid solution but with much reduced sharpness and higher T_{MI} as the Nd content increased.[10] Therefore, we suspected that the Sm ion, probably due to its size coupled with that of Sr, plays a crucial role in displaying the sharp MI-transitions in these compounds.

Tomioka *et al.* studied the MR behavior of $Sm_{0.6}Sr_{0.4}MnO_3$.[11,12] This compound shows almost the same feature as $(Nd_{1-y}Sm_y)_{0.5}Sr_{0.5}MnO_3$ (y=0.938) but somewhat less drastically. A study on $Sm_{1-x}Sr_xMnO_3$ for x=0.33 and 0.40 shows that these also have rather sharp MI-transitions and x=0.2 and 0.55 compounds show semiconducting behavior to the low temperature.[13,14] However, there has been no systematic studies on this system. In this paper, we report the MI transitions in the $Sm_{1-x}Sr_xMnO_3$ ($0.35 \leq x \leq 0.5$) series and the low field MR properties of the x=0.4 member.

$Sm_{1-x}Sr_xMnO_3$ (x=0.35, 0.375, 0.40, 0.425, 0.45, 0.475, 0.5) samples were prepared by calcining stoichiometric mixtures of Sm_2O_3, $SrCO_3$ and Mn_2O_3 at 1000 °C for 10 hour and sintered at 1450-1500 °C for 50-100 hour in air. The single phase nature of the samples were confirmed by indexing their X-ray powder patterns by orthorhombic perovskite structures with the space group Pbnm. The resistance and the magnetization data were obtained by the standard four probe method and on a SQUID magnetometer, respectively.

Figure 1 shows the temperature dependency of resistivity of the compounds in the $Sm_{1-x}Sr_xMnO_3$ system. All the samples in the x-range studied in this study exhibited sharp MI transitions similar to those of $(Nd,Sm)_{0.5}Sr_{0.5}MnO_3$. T_{MI} values varied with x peaking at x=0.45 with 135 K close to the reported value of about 125 K.[11,12] The peak shape in the resistivity *vs.* temperature plot for x=0.4 member is most asymmetric with a steep rise and a gradual decrease with increasing temperature just below and above T_{MI}, respectively. Tokura *et al.*[9] attributed the asymmetric peaks in their $(Nd,Sm)_{0.5}Sr_{0.5}MnO_3$ samples to the first order transition with charge ordering which is often found in other perovskite oxides particularly with the oxidation state of +3.5 for Mn. In their study, however, there was no evidence provided to prove the occurrence of charge ordering. However, our data show that the asymmetric nature of the resistivity vs. temperature does not necessarily have to accompany any particular Mn oxidation state. In fact, as x approaches 0.5 beyond 0.45 the peak shape becomes more symmetric (Figure 1). We believe the asymmetry comes from a certain type of lattice distortion due to the A-site cations.

Since we were seeking a compound with both high T_{MI} and a highly asymmetric MI transition peak, we have

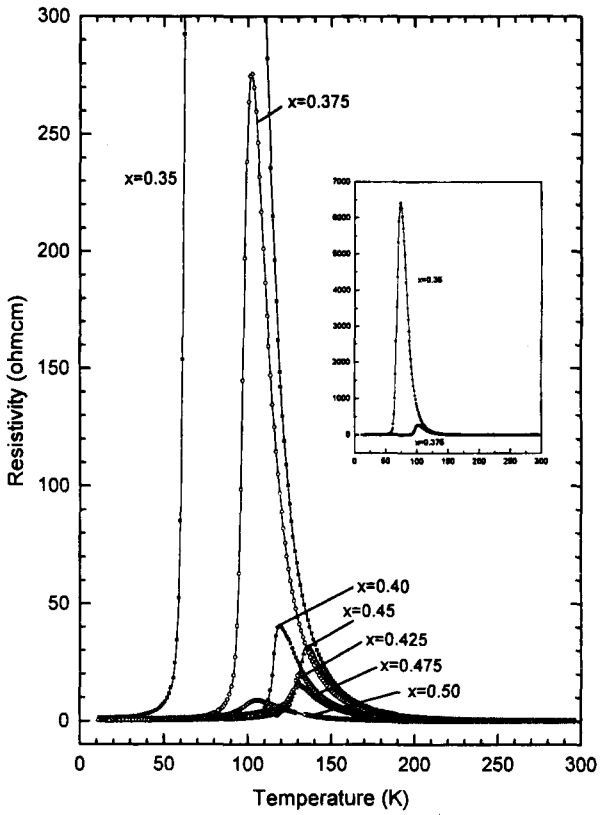

Figure 1. Temperature variations of resistivity of $Sm_{1-x}Sr_xMnO_3$ system for x=0.35, 0.375, 0.40, 0.425, 0.45, 0.475 and 0.50. Inset is an expanded plot to compare the x=0.35 data with the x= 0.375 ones.

chosen the x=0.40 sample for further MR studies. Figure 2 shows the magnetic moment measurement data for $Sm_{0.6}Sr_{0.4}MnO_3$ as a function of temperature under the applied magnetic field of 5000 G. The ferromagnetic ordering temperature of 123 K in the plot is in a good agreement with the T_{MI} (126 K) measured from the resistivity data in Figure 3. T_{MI} value for this comparison was obtained from MR measurements (Figure 3) for which each resistivity measurement was made after the system reached a thermal

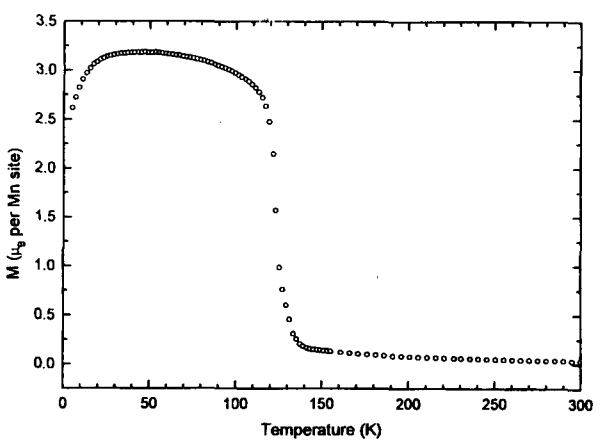

Figure 2. Temperature variations of magnetization for $Sm_{0.6}Sr_{0.4}MnO_3$ under an applied magnetic field of 5000 G.

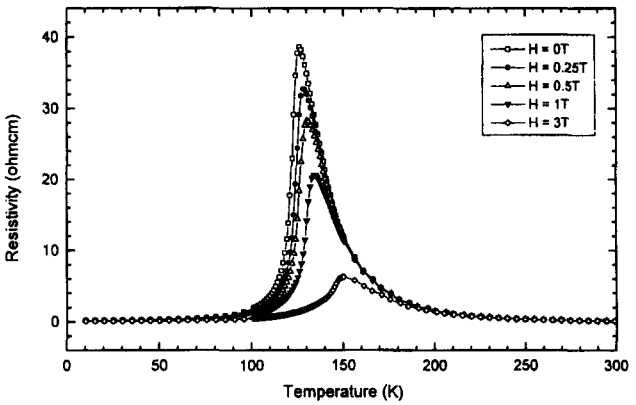

Figure 3. Temperature variations of resistivity of $Sm_{0.6}Sr_{0.4}MnO_3$ under various applied magnetic field strengths.

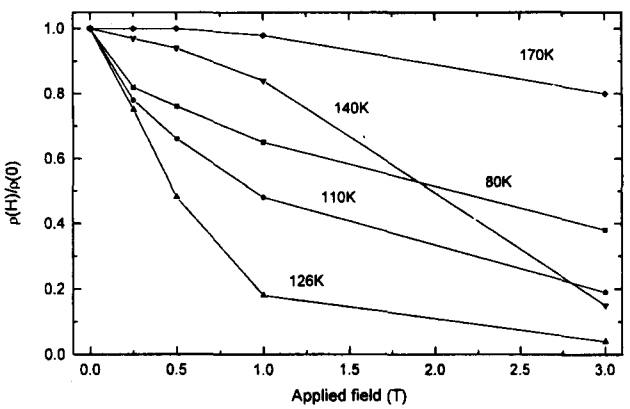

Figure 4. Normalized resistivity of $Sm_{0.6}Sr_{0.4}MnO_3$ as a function of applied magnetic field at various temperatures.

equilibrium which condition is close to those of the SQUID measurements. The resistivity *vs.* temperature data in Figure 1 were obtained with rather fast temperature sweeps that might cause errors in temperature readings. The saturated magnetic moment in the ferromagnetic regime is 3.2 μ_B per Mn site which is close to the fully spin polarized state (3.6 μ_B). Below about 20 K, the magnetic moment is reduced slightly probably indicating a charge ordering transition or an antiferromagnetic behavior due to the ordering of Sm moments..

The MR effect as a function of temperature for this sample at different applied fields are shown in Figure 3. As expected from the peak shapes, the MR effect is very large even under low magnetic field. In Figure 4, we show the normalized resistivity of the same sample as a function of applied magnetic field at various temperatures. At T_{MI}, (126 K) the MR effect is very large at low magnetic field. When the applied field was 1T, the resistance decreased by 82% from the zero field resistance and by 96% at 3T. MR ratio defined as $\Delta R/R_H$ in this sample is reached 2490% at 3T at this temperature. Measurements above and below T_{MI}, showed reduced MR ratios.

In conclusion, we have studied the electrical resistivity of the $Sm_{1-x}Sr_xMnO_3$ ($0.35 \leq x \leq 0.5$) series. These compounds had asymmetric and sharp peaks in the resistivity *vs.* temperature plots than other systems. Of these the compound with x=0.4 showed more asymmetric peaks than the others

and its MR effect was very large even under low magnetic field which is the desired feature for application of MR devices. Although unclear at this moment, this paper demonstrates that high MR materials under low magnetic field are possible by controlling the doping level of a certain system.

Acknowledgment. This study was financially supported by the Korean Science and Engineering Foundation (KOSEF 971-0306-050-3).

References

1. Urushibara, A.; Moritomo, Y.; Arima, T.; Asamitsu, A.; Kido, G.; Tokura, Y. *Phys. Rev. B* **1995**, *51*, 14103.
2. Bae, S.-Y.; Wang, S. X. *Appl. Phys. Lett.* **1996**, *69*, 121.
3. Xiong, G. C.; Bhagat, S. M.; Li, Q.; Dominguez, M.; Ju, H. L.; Greene, R. L.; Venkatesan, T. *Solid State Commun.* **1996**, *97*, 599.
4. Schiffer, P.; Ramirez, A. P.; Bao, W.; Cheong, S.-W. *Phys. Rev. Lett.* **1995**, *75*, 3336.
5. Helmolt, R.; Wecker, J.; Holzapfel, B.; Schultz, L.; Samwer, K. *Phys. Rev. Lett.* **1993**, *71*, 2331.
6. Jia, Y. X.; Lu, Li; Khazeni, K.; Crespi, V. H.; Zettl, A.; Cohen, M. L. *Phys. Rev. B* **1995**, *52*, 9147.
7. Jia, Y. X.; Lu, Li; Khazeni, K.; Yen, D.; Lee, C. S.; Zettl, A. *Solid State Commun.* **1995**, *94*, 917.
8. Kwon, Y. U.; Chi, E. O.; Kang, J. K.; Hur, N. H. *J. Appl. Phys.* **1997**, *82*, 1.
9. Kuwahara, H.; Tomioka, Y.; Moritomo, Y.; Asamitsu, A.; Kasai, M.; Kumai, R.; Tokura, Y. *Science* **1996**, *272*, 80.
10. Tokura, Y.; Kuwahara, H.; Moritomo, Y.; Tomioka, Y.; Asamitsu, A. *Phys. Rev. Lett.* **1996**, *76*, 3184.
11. Tokura, Y.; Tomioka, Y.; Kuwahara, H.; Asamitsu, A.; Moritomo, Y.; Kasai, M. *J. Appl. Phys.* **1996**, *79*, 5288.
12. Tomioka, Y.; Kuwahara, H.; Asamitsu, A.; Kasai, M.; Tokura, Y. *Appl. Phys. Lett.* **1997**, *70*, 3609.
13. Caignaert, V.; Maignan, A.; Raveau, B. *Solid State Commun.* **1995**, *95*, 357.
14. Kasai, M.; Kuwahara, H.; Tomioka, Y.; Tokura, Y. *J. Appl. Phys.* **1996**, *80*, 6894.

Dimerization of β-Iodo-α,β-unsaturated Enones by Samarium(II) Iodide†

Han-Young Kang*‡, Mi Soon Park‡, Bok-Nam Park‡, and Hun Yeong Koh†

‡*Department of Chemistry, Chungbuk National University, Cheongju, Chungbuk 361-763, Korea*
†*Division of Applied Science, Korea Institute of Science and Technology, P.O. Box 131, Cheongryang, Seoul 130-650, Korea*
Received September 8, 1997

Alkene-alkene coupling reactions mediated by an organometallic species have been a subject of intense research interests in organic synthesis.[1] A particular case is the dimerization reaction involving the bond formation between sp^2 carbon centers. Besides the classical Ulmann coupling, many methods of alkene-alkene dimerization using a copper species have been known. Methods using other metals including Ni, Pt, Pd, and Rh have also been reported. Some of the representative substrates used for these dimerization processes are alkenyl halides, alkenylboranes, alkenylmercury species, and alkenylstannes.

Since the pioneering investigation by Kagan and coworkers, samarium(II) iodide has been a useful reagent in synthetic organic chemistry because it promotes various organic transformations.[2] Kagan and other research groups have also reported the coupling reaction of acyl halides mediated by samarium(II) iodide to produce α-diketones or α-ketols.[3] In the presence of ketones and aldehydes, the addition of an acyl moiety to the carbonyl group has been also observed. An acylsamarium species, $RC(O)\text{-}SmI_2$, has been suggested as the key intermediate. This species, then, reacts with electrophiles such as acyl halides, aldehydes, and ketones.

†Dedicated to Professor Yoshito Kishi on the occasion of his 60th birthday.

Since the formation of an acylsamarium species as the key intermediate has attracted attention, we have been interested in the reactions of β-halo-α,β-unsaturated enones in the presence of samarium(II) iodide. These compounds can be considered as vinylogous acyl halides (eq. 1). The formation of a vinylogous acylsamarium species would be of interest with respect to the preparation of coupled products bearing an interesting structural unit.

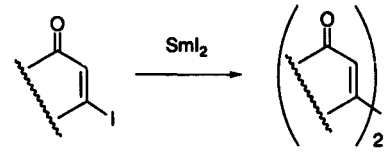

(1)

The necessary β-iodo-α,β-unsaturated enones are easily prepared by the methods reported in the literature.[4] Results of samarium(II) iodide-promoted reactions of β-iodo-α,β-unsaturated enones are summarized in Table 1.

As expected, the dimerization of the starting β-iodo-α,β-unsaturated enones occurred to give the corresponding conjuguated 1,6-ketones (entries 1-6).[5] The six-membered ring cases are more efficient substrates than the five-membered cyclic compounds.[6] The exocyclic β-iodo-α,β-enones also provided the dimerization products efficiently (entries 7-9).